land

MDPI

Article

Forecasting of Grasslands Distribution on Mount Zireia Using Ecological Niche Modeling and Future Climatic Scenarios

Maria Karatassiou [1,*], Afroditi Stergiou [1], Dimitrios Chouvardas [1], Mohamed Tarhouni [2] and Athanasios Ragkos [3]

[1] Laboratory of Rangeland Ecology, School of Forestry and Natural Environment, Aristotle University of Thessaloniki, P.O. Box 286, 54124 Thessaloniki, Greece; afroster@for.auth.gr (A.S.); xouv@for.auth.gr (D.C.)
[2] Pastoral Ecosystems Spontaneous Plants and Associated Microorganisms Laboratory, Arid Regions Institute, University of Gabes, Route of Djerba km 22.5, Medenine 4100, Tunisia; medhtarhouni@yahoo.fr
[3] Agricultural Economics Research Institute, Hellenic Agricultural Organization—DIMITRA, Kourtidou 56–58, 11145 Athens, Greece; ragkosagrecon@gmail.com
* Correspondence: karatass@for.auth.gr; Tel.: +30-2310992302

Abstract: Grassland ecosystems cover a high percentage of the terrestrial habitats of Earth and support the livelihood and well-being of at least one-fifth of the human population. Climate change and human activities are causing increasing pressure on arid and semi-arid regions. Land use/cover change significantly affects the function and distribution of grasslands, showing diverse patterns across space and time. The study investigated the spatial distribution of grasslands of Mount Zireia (Peloponnesus, Greece) using MaxEnt modeling based on CMIP6 models (CNRM-CM6 and CCMCC-ESM2) and two Shared Socioeconomic Pathways (SSP 245 and SSP 585) covering the period of 1970–2100. The results from the current (1970–2000) and several future periods (2020–2100) revealed that the MaxEnt model provided highly accurate forecasts. The grassland distribution was found to be significantly impacted by climate change, with impacts varying by period, scenario, and climate model used. In particular, the CNRM-CM6-1 model forecasts a substantial increase in grasslands at higher elevations up to 2100 m asl. The research emphasizes the importance of exploring the combined impacts of climate change and grazing intensity on land use and cover changes in mountainous grasslands.

Keywords: MaxEnt model; Shared Socioeconomic Pathways; land use/cover change; climate change

Citation: Karatassiou, M.; Stergiou, A.; Chouvardas, D.; Tarhouni, M.; Ragkos, A. Forecasting of Grasslands Distribution on Mount Zireia Using Ecological Niche Modeling and Future Climatic Scenarios. *Land* **2024**, *13*, 2126. https://doi.org/10.3390/land13122126

Academic Editor: Yongheng Gao

Received: 20 October 2024
Revised: 3 December 2024
Accepted: 6 December 2024
Published: 8 December 2024

1. Introduction

Land use/cover change (LUCC) and climate change are the two main categories of environmental changes at both a regional and a global scale [1]. LUCC is described as changing patterns in a specific area over time and space due to different variables, endangering both biological diversity and ecological systems [2–5]. Intense human activities and land abandonment result in LUCC which in turns reduces biodiversity, leads to habitat loss and degradation, and causes landscape isolation, fragmentation, or homogenization [6–8]. In addition, the provision and values of certain ecological services have been modified as a result of LUCC [9,10]. A significant quantity of data are needed to study LUCC and to develop strategies for the sustainable management of natural resources [5,11].

The climate is one of the most important environmental factors affecting LUCC [12–15]. There is no doubt that the climate at the global scale is getting warmer, and many of the changes observed since the 1950s have not been seen for decades or centuries [16], often resulting in extreme weather phenomena and climate patterns, leading to the extinction of species and significant modifications to their habitats and niches [17,18]. Forecasts suggest that by 2100, about 51% of the current flora species will lose half of their geographic distribution [19,20]. Through land use modeling, conservation activities can be efficiently targeted to anticipate the impact of climate change on LUCC [21].

Integrating spatial and temporal models into projections of LUCC is essential for understanding historical patterns and present conditions and making informed decisions for future scenarios [22]. The state-of-the-art machine learning model MaxEnt [23] is regularly used in distribution modeling [24–26]. MaxEnt has been extensively utilized in forecasting the potential geographic range of species and their nonlinear connections between environmental factors and documented sites [27–30]. It has been increasingly used in predicting forest fires [31,32], cultural ecosystem services [1,33], and the impact of human pressures on land use [27,34]. However, its utilization in predicting land uses still needs to be improved [35]. This method is useful for forecasting the full potential geographic distribution of a species (the fundamental environmental niche), but not its actual distribution, which might be limited due to competition, barriers, or human-induced modification of the environment. This approach is also used to determine the relative importance of various environmental variables for species distribution and the relative suitability of different areas as potential habitats [23,36]. Classifications of land cover are studied in the same way as species or habitats [37].

Grassland ecosystems cover about 20–26% of the Earth's land area [38] and support the livelihood and general well-being of one-fifth of the human population [39,40]. These ecosystems provide grazing areas for livestock [38,41], habitats for wildlife [39], and contribute to the provision of ecosystem services, such as environmental protection, water storage, carbon sequestration, and in situ conservation of plant genetic resources [42–44]. Despite their crucial role and the significant ecosystem services they provide, the importance of grasslands is often overlooked [45,46].

Climate and human activities are both key factors in the development and longevity of grasslands [44]. Grazing is acknowledged as a crucial element in protecting grassland habitats, enhancing biodiversity and ecosystem function. Nonetheless, grasslands are still at great risk from multiple sources, such as climate change, land use, soil degradation, nutrient loss, fires, habitat fragmentation, and human activities [44,47–49]. Precipitation and grazing play significant roles in determining species diversity and overall ecosystem functioning in grassland ecosystems and especially overgrazing can lead to severe habitat loss and degradation [38,50,51], which is estimated from 10–20% to 70–80% [52]. Moreover, they have been exposed to increased hazards due to extensive use and deterioration [53–55]. Elevation also has a major impact on climatic conditions and land formation, which then affects the availability of resources, plant growth regulators, and species diversity [56,57]. The above dynamics have a severe effect also in the Mediterranean basin, where 10–20% of the total area is covered by grasslands distributed across various elevation zones, each playing a unique ecological role, supporting important ecosystem services, and facing distinct environmental challenges [58].

In Greece, the highest percentage of grasslands is located in the middle and high (mountainous) elevation zones (32 and 51%, respectively) [59]. Mountainous grasslands offer excellent grazing areas for transhumant livestock and play a vital role in preserving biodiversity and landscapes, as well as in mitigating climate change and regulating water resources [60,61]. Transhumance is a type of pastoralism where animals are moved periodically between different elevation zones to take advantage of seasonally available grazing resources [61]. Nonetheless, these ecosystems are particularly vulnerable to the impacts of climate change, including altered rainfall patterns and rising temperatures [62] and the cumulative risk of desertification. The importance of integrated management strategies to maintain the ecological integrity of grasslands is amplified by the complex interactions between land use (human activities) and climate over space and time [63] in the face of ongoing environmental change. To the best of our knowledge, the Maxent model has not been applied to study the impact of climate change on land use, particularly grasslands, in the Mediterranean region.

The aim of the current study was to evaluate the effects of climate change on the structure and distribution of the grasslands in a Mediterranean mountain. We selected a typical Mediterranean mountain, Mt Zireia, lying on the northeast part of the Peloponnese,

Greece, and we tested two different climate models and scenarios by utilizing the MaxEnt modeling approach. From the Shared Socioeconomic Pathways (SSPs), we tested two scenarios: the SSP245 as intermediate and SSP585 as pessimistic, and we projected forecasts up to 2100.

2. Materials and Methods

2.1. Study Area

The study area is Mount Zireia with an altitudinal range of 310 to 2374 m a.s.l. It is located in the prefecture of Korinthos, 115 km west of Athens, and includes approximately 39,761.57 ha (Figure 1). The Natura2000 network comprises more than two thirds of the study area (Natura 2000). The lakes Stymfalia (15.285 ha) to the south and Doxa (48 ha) to the west are the primary hydrological basins in the region (Figure 1) that highly affect microclimatic conditions. The climate is categorized as Mediterranean, featuring mild winters and arid, extremely hot summers, in line with Emberger's bioclimatogram and classified as Csa in the Köppen–Geiger system (http://www.en.climate-data.org, accessed on 23 May 2022). Over the last 60 years, the mean annual temperature has fluctuated from 12.59 to 15.55 °C, and the mean annual precipitation varied from 418.62 mm to 1056 mm [64]. Agriculture and livestock production are the primary economic activities in the region [60]. The traditional transhumant livestock system has been present in the study area for many years but has experienced a significant decline in recent decades.

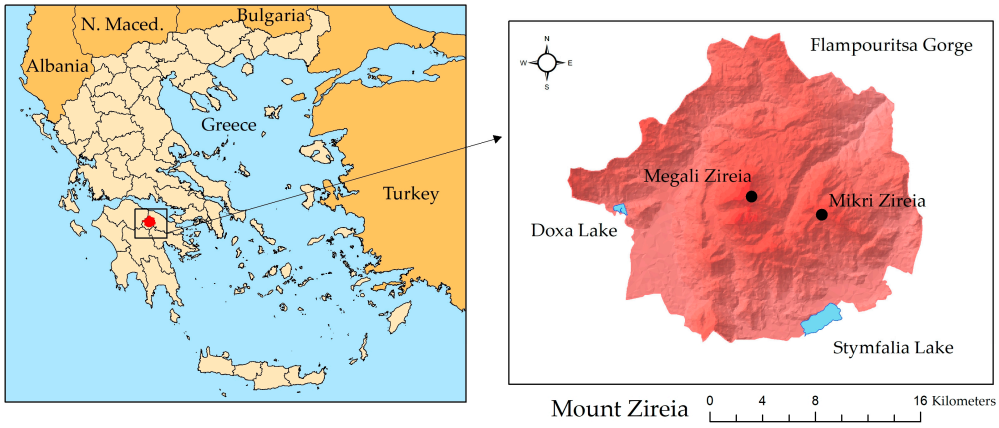

Figure 1. Geographical location of the study area.

2.2. Current Land Use/Land Cover Data

The land use/cover classification process was carried out mainly by using visual photo-interpretation techniques and digital processes in satellite images from Google Earth Pro v.7.3 software for 2017, 2019 and 2020 (georeferenced to the Hellenic Geodetic Reference System 1987-HGRS87), according to a procedure used in the study by Chouvardas et al. [8]. The above analysis was processed using ArcGIS 10.8, resulting in the creation of a digital LULC map for 2020. Among the various land use categories identified—such as agricultural areas, grasslands, open shrublands, dense shrublands, silvopastoral areas, forests, barren areas, urban areas, and lakes—this study focused specifically on the geographical distribution of grasslands. These grasslands, classified as discontinuous, covered an estimated area of 5893.51 hectares, representing 14.8% of the total study area.

Initially, a grid of 1000 m cell size was created (fishnet) in the shapefile format using ArcGIS 10.8. A total of 234 grassland distribution points were collected as dependent variables in the MaxEnt model. The samples' longitude and latitude coordinates were recorded in the Excel database and converted to CSV format for developing the MaxEnt model.

2.3. Environmental Variables for Model Fitting

Three topographic (elevation, slope, and aspect) and nineteen bioclimatic variables (bio1–bio19), reflecting seasonal changes in temperature and precipitation, with 30 s (ca.

1 km) spatial resolution were selected (Table 1) for developing an ecological niche model. The elevation in Digital Elevation Map (DEM) format was downloaded from the Jet Propulsion Laboratory of NASA (Aster GDEM v3, https://asterweb.jpl.nasa.gov/gdem.asp, accessed on 8 February 2022), while the aspect and slope were extracted from the elevation map using ArcGIS 10.8. The bioclimatic variables were obtained from the Wordclim Dataset [65] (http://www.worldclim.org, accessed on 8 February 2022). Twelve soil variables with 250 m spatial resolution and a depth of 0–5 cm except for soil organic carbon content, whose depth was set by default at 0–30 cm, were also selected and downloaded from the Soil Grids website (https://soilgrids.org, accessed on 15 January 2023) (Table 1). These layers were converted into ASCII raster format and given the same geographic projection, extent, and cell size for utilization in the MaxEnt model [19]. We included all 34 variables in our models at the same time following Feng et al.'s [66] observation that high collinearity poses a lesser issue for machine learning techniques compared to statistical models [67,68]. Furthermore, removing variables with high correlations does not improve Maxent models since the algorithm can handle redundant variables and reduce the effects of variable collinearity during model training [66]. Moreover, multicollinearity can lead to response curves that are not reliable because the impact of one factor is mixed up with its correlation to other factors, making it challenging to determine the actual effect of each predictor [69,70].

Table 1. Environmental variables for the geographic distribution of grasslands in Mount Zireia.

Type	Abbreviation	Description	Units
Bioclimatic	bio1	Mean Annual Temperature	°C
	bio2	Mean Diurnal Range (Mean of monthly (max temp-min temp))	°C
	bio3	Isothermally (Bio2/Bio7) (×100)	°C
	bio4	Temperature Seasonality (standard deviation ×100)	°C
	bio5	Max Temperature of Warmest Month	°C
	bio6	Min Temperature of Coldest Month	°C
	bio7	Temperature Annual Range (Bio5–Bio6)	°C
	bio8	Mean Temperature of Wettest Quarter	°C
	bio9	Mean Temperature of Driest Quarter	°C
	bio10	Mean Temperature of Warmest Quarter	°C
	bio11	Mean Temperature of Coldest Quarter	°C
	bio12	Annual Precipitation	mm
	bio13	Precipitation of Wettest Month	mm
	bio14	Precipitation of Driest Month	mm
	bio15	Precipitation Seasonality	mm
	bio16	Precipitation of Wettest Quarter	mm
	bio17	Precipitation of Driest Quarter	mm
	bio18	Precipitation of Warmest Quarter	mm
	bio19	Precipitation of Coldest Quarter	mm
	elevation_aster	elevation	m
Topographic	slope_aster	slope	%
	aspect_aster	aspect	°

Table 1. *Cont.*

Type	Abbreviation	Description	Units
Soil	bulk density	Bulk density of the fine earth fraction	cg/cm^3
	cationexchcap	Cation exchange capacity of the soil	mmol(c)/kg
	coarsefragm	Volumetric fraction of coarse fragments (>2 mm)	cm^3/dm^3 (vol‰)
	claycontent	Proportion of clay particles (<0.002 mm) in the fine earth fraction	g/kg
	nitrogen	Total nitrogen (N)	cg/kg
	phwater	Soil pH	pH × 10
	sand	Proportion of sand particles (>0.05 mm) in the fine earth fraction	g/kg
	silt	Proportion of silt particles (≥0.002 mm and ≤0.05 mm) in the fine earth fraction	g/kg
	soilorgcarb	Soil organic carbon content in the fine earth fraction	dg/kg
	orgcarbden	Organic carbon density	hg/m^3
	worldrbssoilg	World reference base (2008) soil groups (an international soil classification system for naming soils)	
	soilorcarbst	Organic carbon stocks	

2.4. Environmental Variables for Forecasting Model

From the Climate Model Intercomparison Project Phase 6 (CMIP6), we selected the models CNRM-CM6 [71] and CCMCC-ESM2 [72,73] to forecast the future grassland distribution on Mt Zireia. We selected four future periods (2021–2040, 2041–2060, 2061–2080, and 2081–2100) in addition to historical data (1970–2000) (http://www.worldclim.org, accessed on 8 February 2022). The CMIP6 includes various scenarios known as SSPs, representing emission scenarios based on varying socioeconomic assumptions. The SSPs are identified from SSP126 to SSP585 (https://climate-scenarios.canada.ca/?page=cmip6-overview-notes, accessed on 8 February 2022). In this study, the SSP245 and the SSP585 were selected as the intermediate scenario and as the pessimistic GHG emissions scenario, respectively, to predict the average suitable distribution areas of grasslands on Mt Zireia from 2021 to 2100 [74,75].

2.5. MaxEntropy Modeling

We used MaxEnt software (version 3.4.3) to simulate the potential current and future distribution of grasslands and identify the environmental factors that impact their distribution [23,76]. MaxEnt employs the maximum entropy algorithm and land occurrence to predict the probability of land use [77]. For model calibration and assessment, 75% of the data was utilized for training, while the remaining 25% was used to test the model's predictive capabilities for grassland distribution [78]. The automatic settings were configured for linear, quadratic, product, threshold, and hinge. The model was set up according to Tavanpour et al. [79], Saha et al. [36], and Ramasamy et al. [80] using 10,000 random background points as pseudo-absence throughout the study area and by regularizing multiplier 1 and 500 iterations with a 0.050 convergence threshold. The output of the Cloglog was utilized in the MaxEnt model to create a continuous map showing the predicted probability of presence ranging from 0 to 1. The test was conducted by excluding each variable systematically to evaluate the significance of environmental variables [78,81]. The Jackknife tests in Maxent were used to measure the dominant environmental variables contributing to grassland distribution. The software algorithm runs a maximum iteration of 500 of these

processes and 0.00001 of convergence threshold. The Receiver Operating Characteristic (ROC) shows the corresponding values for Specificity (Fractional Predicted Area on the horizontal axis) and sensitivity (Omission Rate on the vertical axis), with one point for each unique threshold [82]. The MaxEnt model's prediction accuracy is determined by the Area Under the Curve (AUC) from the ROC [23,65,83,84]. The AUC values range from 0 to 1. Fielding [85] states that the model's predictive power increases with a greater numerical value. An AUC value of less than 0.5 indicates performance poorer than chance, whereas an AUC value of more than 0.75 indicates high performance, and 0.5 suggests a forecast similar to random chance [86]. The Maxent outputs were in ASCII format, and ArcMap 10.8 was used to analyze and visualize the final forecasting maps [65]. The grassland forecasting map was classified into three classes following Coban et al. [84] based on potential suitable distribution: marginal 0.25–0.5, moderate 0.5–0.75, and high >0.75. The area of the three vegetation classes was then computed.

3. Results

3.1. Evaluations of the Model and Its Importance of Variables Under Current Climatic Conditions

The AUC values for the training and test data showed that our modeling approach's prediction accuracy for 1970–2000 was 0.864 and 0.786, respectively (Figure 2). The Jackknife test indicated that from all the independent examined environmental variables, the distribution of grasslands was mostly influenced by bio8, bio6, bio12, bio19, and elevation (Figure 3).

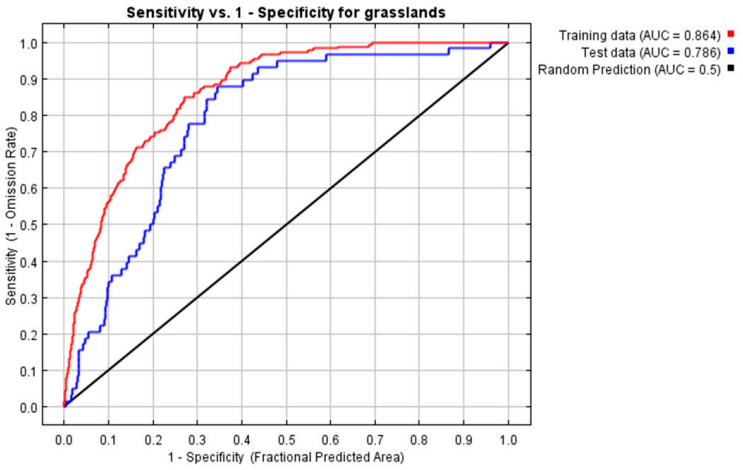

Figure 2. Area Under the Curve (AUC) value for the historical data, period 1970–2000.

3.2. Model Evaluations and Jackknife Test of Variables for Future Periods Under Different Climate Models and Scenarios

All AUC values for all future periods were >0.858 (Table 2). The climate model CCMCC-ESM2 and the pessimistic scenario (SSP585) for the period 2061–2080 demonstrated the highest AUC value (0.883), while the SSP585 from CNRM-CM6-1 appears with the lowest AUC value (0.859) for the period 2081–2100.

Table 2. The values of Area Under the Curve (AUC) for the future periods (2021–2040, 2041–2060, 2061–2080, 2081–2100) and the two CMIP6 climate models (CNRM-CM6-1 and CCMCC-ESM2) under the scenarios SSP245 and SSP585.

Future Period	CMIP6 Climatic Models			
	CNRM-CM6-1		CCMCC-ESM2	
	SSP245	SSP585	SSP245	SSP585
2021–2040	0.874	0.870	0.883	0.871
2041–2060	0.870	0.874	0.860	0.868

Table 2. *Cont.*

Future Period	CMIP6 Climatic Models			
	CNRM-CM6-1		CCMCC-ESM2	
	SSP245	SSP585	SSP245	SSP585
2061–2080	0.874	0.873	0.868	0.883
2081–2100	0.866	0.859	0.869	0.866

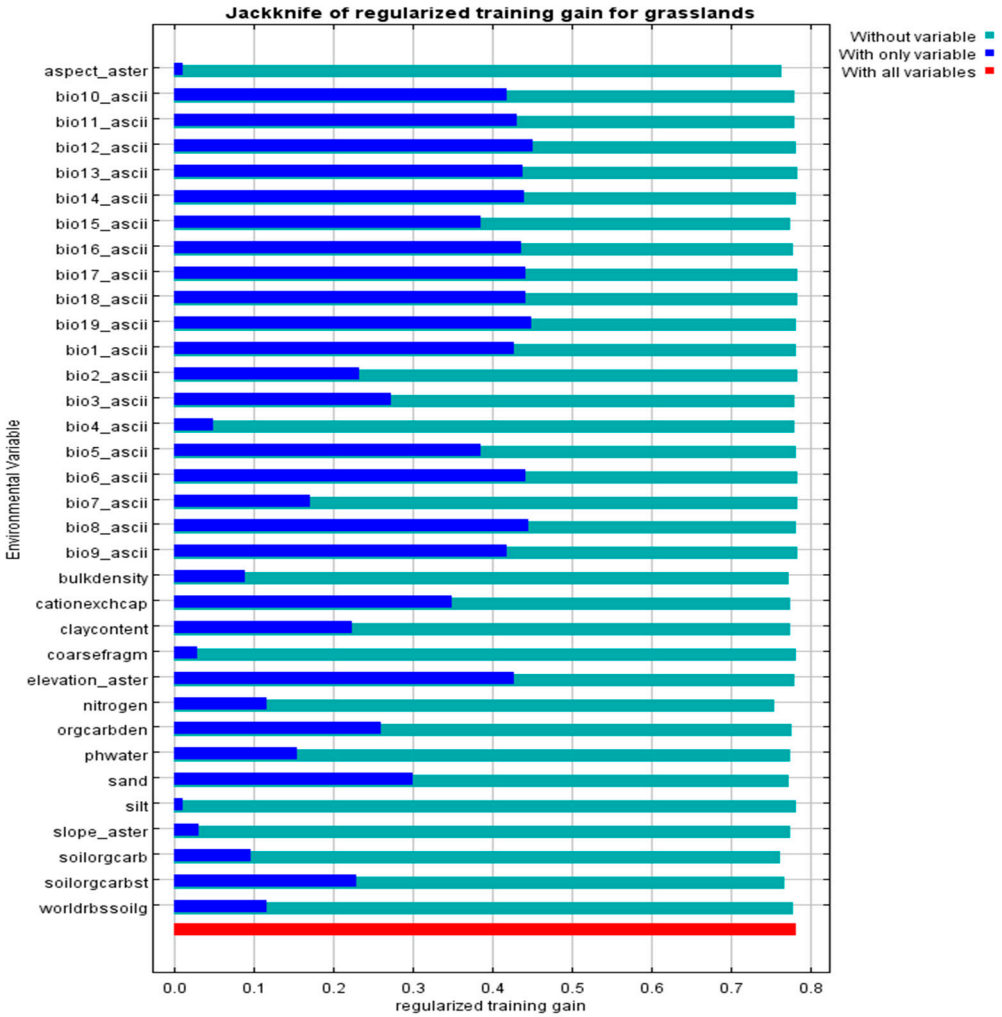

Figure 3. The relative predictive power for grasslands of the thirty study environmental variables is based on the Jackknife values of regularized training gain in the MaxEnt model.

The Jackknife test demonstrated that under the CNRM-CM6-1 model and intermediate SSP245 scenario for all future periods, the environmental variables that contributed the most to the model performance were bio12, bio6, and elevation (Figure 4). Moreover, the distribution of grasslands could be predicted for the periods 2021–2040 and 2041–2060 based on bio14, bio17, bio18, and bio19 (Figure S1a,b). The bio8 was only significant for the period 2041–2060 (Figure S1b). The Jackknife test also indicated that bio8 and bio16 were significant variables for predicting the distribution of grasslands for the years 2061–2080 (Figure S1c), while for 2081–2100, bio19 and bio14 were the most significant ones (Figure S1d).

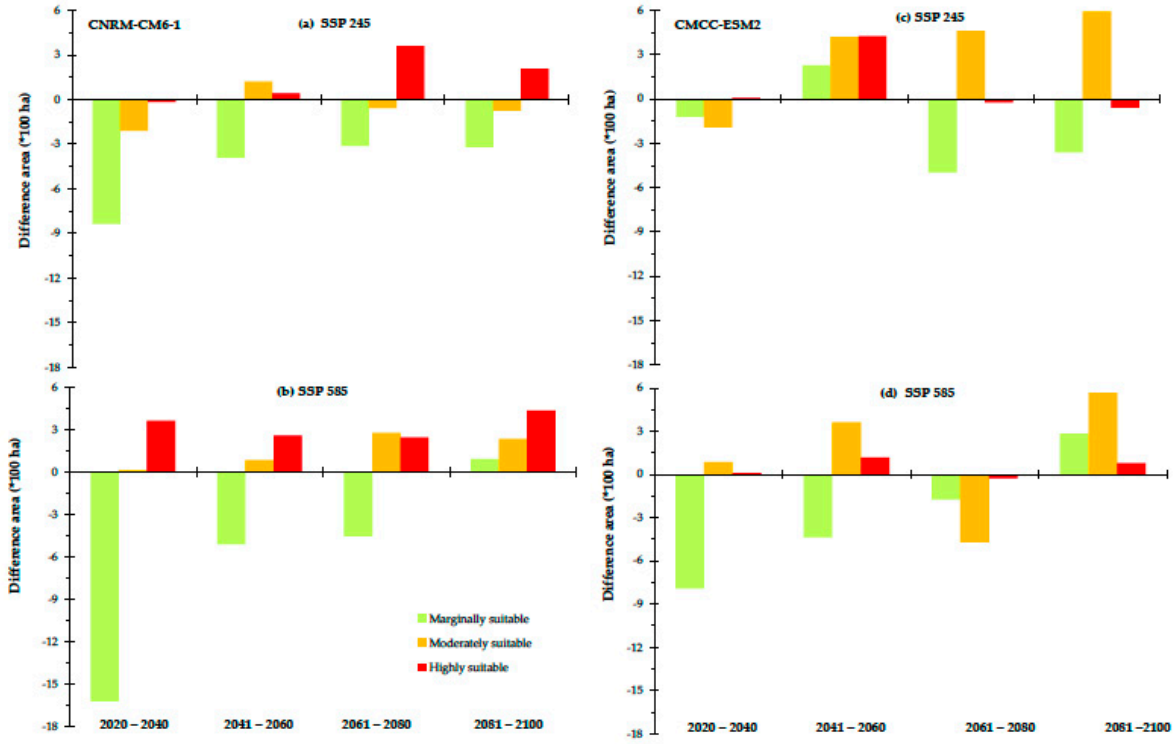

Figure 4. Potential changes in the grasslands' areas according to the suitability classes for the climate models CCNRM-CM6-1 and CMCC-ESM2 and SSP245 (**a**,**c**) and SSP585 (**b**,**d**) scenarios, respectively.

Under the CCMCC-ESM-2 climate model and the intermediate SSP245 scenario for all future periods, the Jackknife test highlighted bio12, bio6, bio8 bio14, and elevation as the environmental variables that contributed the most to model performance (Figure S2). However, for the periods 2021–2040 and 2041–2060, the distribution of grasslands could be predicted with greater accuracy based on bio17, bio18, and bio19 (Figure S2a,b). For the periods 2061–2080 and 2081–2100, the most significant variables influencing the distribution of grasslands were bio14, bio12, bio 6, and elevation (Figure S2c) as well as bio1, bio9, bio10, bio11, and bio16 were also one of the significant variables for predicting the distribution of grasslands (Figure S2d), respectively.

For all future periods under the climate model CNRM-CM6-1 and the pessimistic scenario, the Jackknife test demonstrated that the environmental variables that contributed the most to the model performance were bio14, bio6, and bio8 (Figure S3). More specifically, for the periods 2021–2040, 2041–2060, and 2061–2080, the Jackknife test showed that bio11, bio12, bio17, bio18, and bio19 were also crucial for predicting the grasslands' distribution (Figure S3a–c). The bio11 was only important for the period 2021–2040 (Figure S3a). Elevation was important in all future examined periods except for 2041–2060 (Figure S3b).

Under the climate model CCMCC-ESM2 and pessimistic (SSP585) scenario, the Jackknife test revealed that bio12 and bio19 were the dominant environmental variables in predicting the future distribution of grasslands (Figure S4). However, for the periods 2021–2040, 2041–2060, and 2061–2080, bio17 and bio18 were also very crucial predictors (Figure S4a–c) while bio16 was only significant in 2021–2040 (Figure S4a). The variables bio8, bio6, and bio14 were important for 2021–2040 and 2061–2080 (Figure S4a,c), whereas bio6 was also one of the most major relatively important variables for 2081–2100 (Figure S4d). Elevation was also an important variable for predicting the grasslands' distribution in all future periods except 2081–2100 (Figure S4d).

3.3. Current and Future Predictions of the Potential Distribution of Grasslands Using Ecological Niche Modeling

The current predictions (1970–2000) for grassland performance on Mt Zireia revealed that 7.9% of the study area showed high performance, 10.9% had moderate performance, and 19.3% displayed poor performance. Additionally, 61.9% of the entire study area was unsuitable for grasslands (Figures 4 and 5).

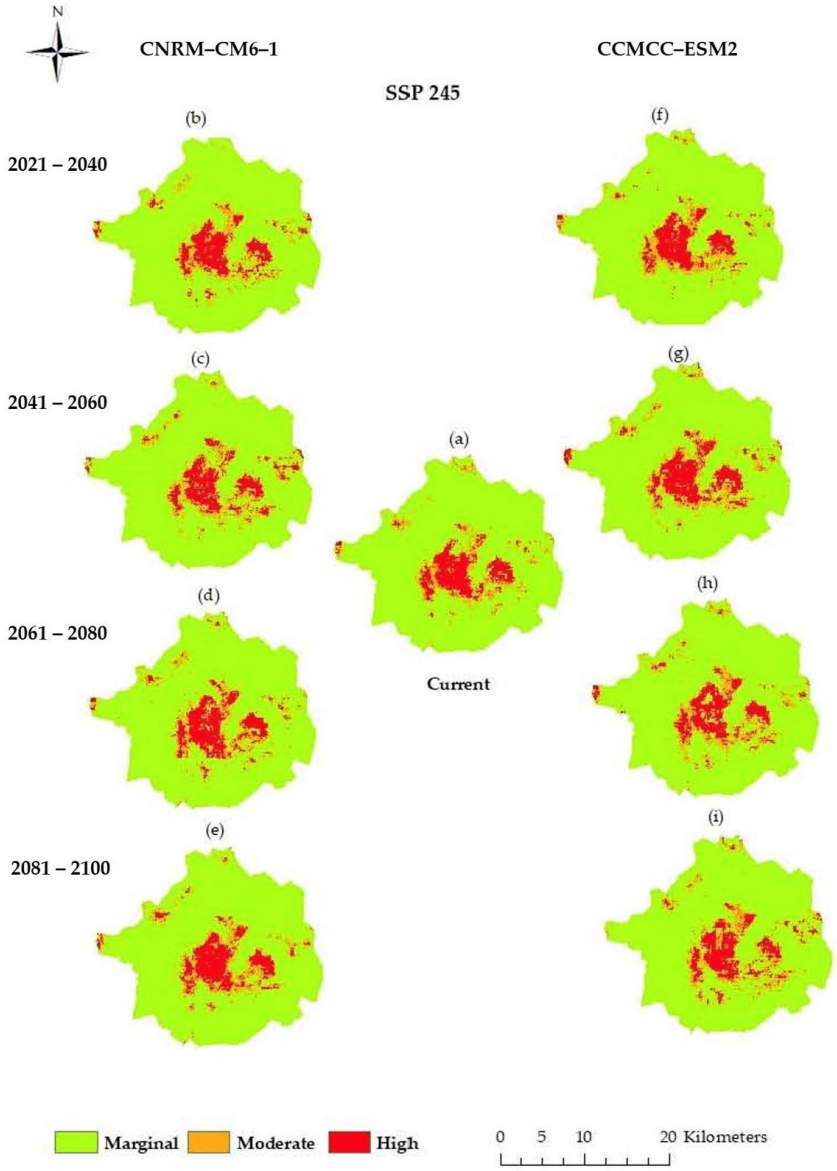

Figure 5. Potential spatial distribution of grasslands for the climate models CNRM-CM6-1 (**b**,**c**,**d**,**e**) and CCMCC-ESM-2 (**f**,**g**,**h**,**i**) under the SSP245 scenario for current (**a**) and future periods from 2020 up to 2100.

According to the predictions for the future of the CNRM-CM6-1 climatic model, there was an expansion of the high suitability area for grasslands in all periods except for 2021–2040 in the SSP245 scenario, which showed a slight decrease (Figures 4–6). Furthermore, the moderately appropriate area increased in all periods in the SSP585 scenario, as opposed to the SSP245 scenario, which increased only during 2041–2060 (Figures 4–6). The area with high suitability displayed variations across time for all upcoming years and both scenarios, with no clear pattern within the CCMCC-ESM2 climate model. The moderate suitable area increased in most periods and scenarios, except for 2021–2040 in the SSP245 scenario and 2061–2080 in the SSP585 scenario (Figures 4–6).

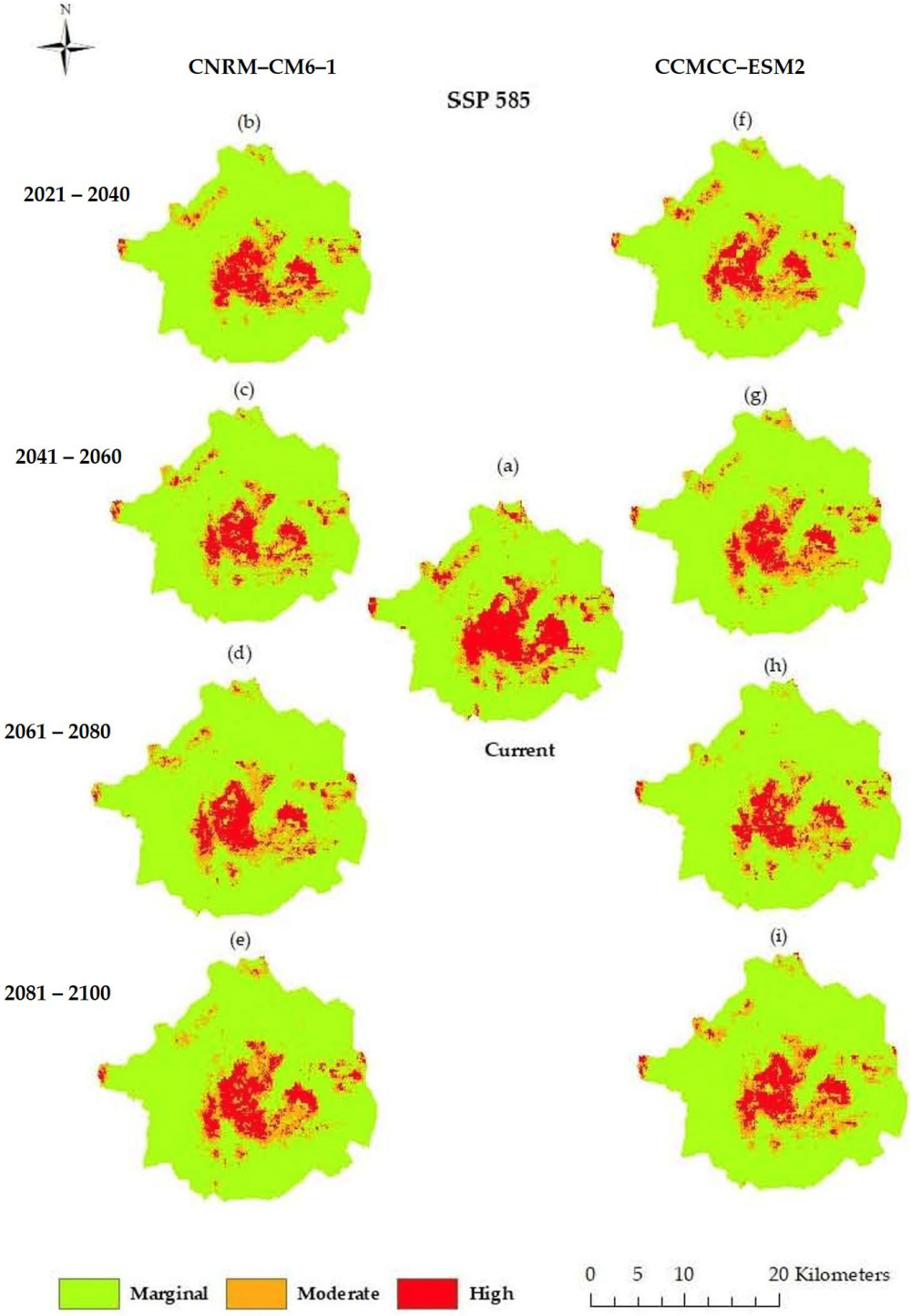

Figure 6. Potential spatial distribution of grasslands for the climate models CNRM-CM6-1 (**b**,**c**,**d**,**e**) and CCMCC-ESM-2 (**f**,**g**,**h**,**i**) under the SSP585 scenario for current (**a**) and future periods from 2020 to 2100.

Figure 7 illustrates the projected distribution of grasslands in four elevation zones based on the CNRM-CM6-1 model's predictions under SSP245 and SSP585 scenarios. The findings showed that elevations above 1200 will experience an increase in grassland area. The increase will be higher in the pessimistic scenario (SSP585).

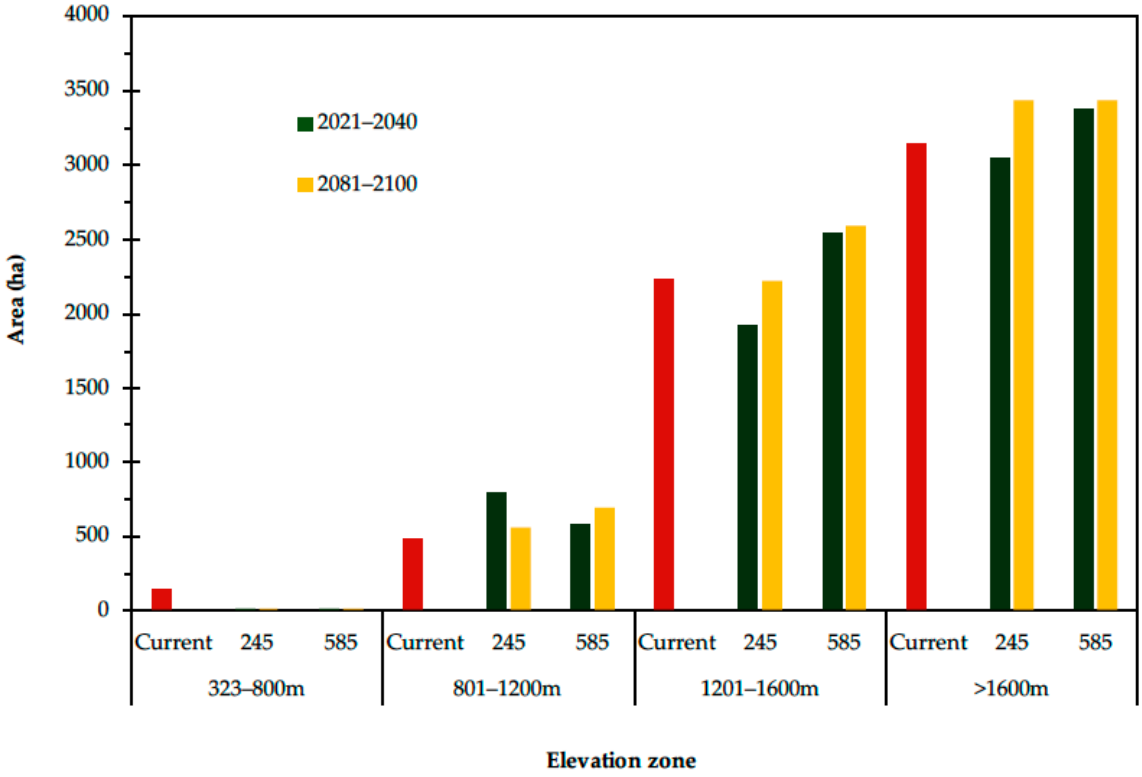

Figure 7. Forecasted current and future areas of grasslands on Mt Zireia by the CNRM-CM6-1 climate model and scenarios in the four elevation zones for current and future periods 2021–2040 and 2081–2100.

4. Discussion

The results of the present study demonstrated that (a) the MaxEnt model was highly accurate under the two examined climate models, (b) climate change strongly impacts the distribution of grasslands on Mt Zireia, (c) forecasting is differentially affected by specific periods, scenarios tested, and climatic models, and (d) the model CNRNM-CM6-1 predicts a substantial increase in grassland up to 2100, especially in elevations higher than 1200 m asl.

The accuracy of MaxEnt was high in forecasting suitable areas for grassland prevalence (AUC values from 0.858 to 0.883). It is widely accepted that AUC values higher than 0.8 demonstrate high performance of the model [68,87–90].

There is no agreement regarding the relative significance of the selection period, scenario, and climatic model as far as the prediction of the MaxEnt model is regarded [91,92]. The predictions of different models under the same scenario for the potentially suitable areas were different. The SSP245 scenario within the CNRM-CM6-1 model showed that the potential highly suitable areas for grassland areas will increase up to 2100 except for the period 2021–2040, while the CCMCC-ESM2 model did not show a clear future trend. On the other hand, in the SSP585 scenario, both models predicted similar changes in the moderately suitable grassland area, showing an increase in all future periods except for 2061–2080 in the CCMCC-ESM2 model. Our results are in agreement with Zhou et al. [65] who found different distribution trends in *Cunninghamia lanceolata* under different models and scenarios. Many studies mentioned that examining the forecasts from various models under the same scenario reveals diverse prediction outcomes [65,93]. The different SSP scenarios, based on different socio-economic patterns and carbon emissions, affected the trend in land use and cover change and were probably influenced not only by radiative forcing but also by unique local development pathways within various societies [93].

In our study, out of the examined environmental variables in the two climate models, annual precipitation (bio12), minimum temperature of the coldest month (bio6), and ele-

vation had the most important effects on the distribution of grasslands. Our results agree with the findings of Zhou et al. [65], Zhang et al. [94], and Yan et al. [76], demonstrating that temperature, precipitation, and temperature changes were the most critical environmental factors. Temperature and precipitation are significant factors for plant growth and phenology, such as the beginning and end of the growing season, timing of flowering, and physiology [95]. Changes in species phenology, as a result of climate change, have been observed to be primarily associated with temperature [95,96], while in arid and semi-arid environments, the seasonal patterns of precipitation can also have a significant impact [97]. According to Bede-Fazekas et al. [91], global climate change is causing a rearrangement of bioclimatic variables worldwide, such as precipitation and temperature timing. Researchers in recent decades have observed a rise in global net primary production because of the prolonged growing season caused by higher temperatures, particularly in mid and northern latitude areas [98]. However, in environments under water stress (arid and semi-arid), the factors influencing the timing and intensity of greenness in response to climate remain uncertain. Variables related to soil did not reveal an important role in grasslands' distribution and probably in the species that participate in their floristic composition [90]. Slope and aspect had a minimal impact on grassland distribution, as other researchers agreed that local topography can only influence microhabitat conditions in comparison to climate and disturbance regimes, which are generally the major determinants of grassland distribution [99], especially in arid and semi-arid environments [100]. On the other hand, the elevation was a significant predictor of grassland performance as is mentioned in other studies [101,102].

The influence of climate change is different in each elevation zone. These mountainous areas are identified as a "hotspot" for climate change, leading to significant impacts on mountain ecosystems, and human communities [103]. In Greece, a higher percentage of grassland occurs in the mountainous zone. However, mountainous grasslands are extensive ecosystems found across the globe, offering a range of economic and cultural benefits [46]. Our results reveal climate- and elevation-related effects, and we predicted a higher increase in mountainous grassland areas under the pessimistic scenario. This could be attributed to the change in temperature and precipitation. Considering the climate model CNRM-CM6-1, under the intermediate scenario, we predict an increase in the minimum temperature of the coldest month (bio6) by 1 °C and 2 °C for the specific periods 2020–2040 and 2081–2100, respectively. A decrease in annual precipitation (bio12) by 20 and 90 mm for the above periods, respectively, is also predicted. Under the pessimistic scenario, the changes in the above bioclimatic parameters were higher. The minimum temperature of the coldest month (bio6) increased by 1.5 °C and 4 °C, and the annual precipitation (bio12) decreased by about 20 and 170 mm for the specific periods 2020–2040 and 2081–2100, respectively (unpublished data). Especially for the mountainous zone, a 100 mm and 190 mm decrease in precipitation is predicted for the periods 2020–2040 and 2081–2100, respectively. Currier and Sala [97] revealed that precipitation impacted the beginning and end of the growing season, while temperature only impacted the start of plant growth. Changes in plant growth patterns can influence the supply of food for livestock, which has an impact on the economy of pastoral communities and especially transhumance [104,105]. The diachronically higher potential distribution of grasslands in the high elevation areas (central part of the study area) can be attributed to an observed trend in recent years called "the mountain effect" [106]. According to this trend, grasslands located at higher elevations exhibit greater resistance to change, primarily due to the traditional practice of vertical transhumance in the region [107] and the challenging soil and climatic conditions in the area [108]. These areas may provide suitable habitats for species migrating to higher altitudes in response to the impacts of climate change [109,110].

Climate change can have intricate effects on grasslands by changing plant competition, growth patterns, productivity, and plant–animal interactions, leading to a decline in forage quality [16]. Grazing is a well-established method of maintaining grasslands, especially in mountainous areas. In most grasslands, precipitation and grazing are key factors

influencing species diversity and ecosystem function [18,57,95,111]. Grazing animals, human activities, soil quality, nutrient depletion, fire, habitat fragmentation, and climate change have a significant impact on grasslands [41,44]. In most grasslands, changes in temperature along with precipitation [112] and grazing [113,114] are the main variables influencing species diversity and ecosystem function [115,116]. The grasslands on Mt Zireia are vital for sedentary and transhumant livestock as they provide necessary forage production from May to October [107]. Nevertheless, in this study, the impact of grazing was not examined. Many studies have demonstrated that grasslands can generate a range of ecosystem services sustainably, even during extreme weather events, if management adapts to changing conditions quickly and effectively [103].

Overall, our study underscores the importance of examining the combined impacts of climate change and grazing intensity on land use and cover changes, particularly in mountainous grassland ecosystems. This research lays the foundation for more in-depth analysis of how climate change affects highland ecosystems. It is crucial for farmers and other stakeholders to understand and adapt to the shifting environmental conditions, ensuring the resilience of these ecosystems. In particular, pastoral agents can play a pivotal role since they are very vulnerable to climate change dynamics, and this calls for systematic mitigation and adaptation actions to ensure their livelihoods. By integrating data and analytical tools, we can improve livestock management strategies and support informed decision-making. This approach not only aids in the sustainable management of land use but also contributes to conservation efforts, providing essential guidance for preserving these vital ecosystems in the face of ongoing climatic challenges.

Supplementary Materials: The following supporting information can be downloaded at: https://www.mdpi.com/article/10.3390/land13122126/s1, Figure S1: Jackknife test of CNRM-CM6-1 model and SSP245 scenario for periods 2021–2040 (a), 2041–2060 (b), 2061–2080 (c), and 2081–2100 (d); Figure S2: Jackknife test of CCMCC-ESM2 model and SSP245 scenario for periods 2021–2040 (a), 2041–2060 (b), 2061–2080 (c), and 2081–2100 (d); Figure S3: Jackknife test for CNRM-CM6-1 model and SSP585 scenario for periods 2021–2040 (a), 2041–2060 (b), 2061–2080 (c), and 2081–2100 (d); Figure S4: Jackknife test for CCMCC-ESM2 model and SSP585 scenario for periods 2021–2040 (a), 2041–2060 (b), 2061–2080 (c), and 2081–2100 (d).

Author Contributions: Conceptualization, M.K., A.S. and M.T.; methodology, M.K. and M.T.; software, M.K., A.S. and D.C.; validation, M.K.; formal analysis, A.S. and D.C.; investigation, M.K., A.S. and D.C., resources, M.K.; data curation, M.K., A.S. and D.C.; writing—original draft preparation, M.K. and A.S.; writing—review and editing, M.K., A.S., D.C., M.T. and A.R.; visualization, M.K.; supervision, M.K.; project administration, M.K.; funding acquisition, M.K. and A.R. All authors have read and agreed to the published version of the manuscript.

Funding: This research is part of the project PASTINNOVA "Innovative models for sustainable future of Mediterranean pastoral systems" financed by the Partnership for Research and Innovation in the Mediterranean Area (PRIMA) program supported by the European Union under the grant agreement No 2113.

Data Availability Statement: The data presented in this study are available in the Figures and Tables provided in the manuscript.

Conflicts of Interest: The authors declare no conflicts of interest.

References

1. He, S.; Su, Y.; Shahtahmassebi, A.R.; Huang, L.; Zhou, M.; Gan, M.; Deng, J.; Zhao, G.; Wang, K. Assessing and mapping cultural ecosystem services supply, demand and flow of farmlands in the Hangzhou metropolitan area, China. *Sci. Total Environ.* **2019**, *692*, 756–768. [CrossRef] [PubMed]
2. Lawler, J.J.; Lewis, D.J.; Nelson, E.; Plantinga, A.J.; Polasky, S.; Withey, J.C.; Helmers, D.P.; Martinuzzi, S.; Pennington, D.; Radeloff, V.C. Projected land-use change impacts on ecosystem services in the United States. *Proc. Natl. Acad. Sci. USA* **2014**, *111*, 7492–7497. [CrossRef]
3. Meyfroidt, P.; Lambin, E.F.; Erb, K.H.; Hertel, T.W. Globalization of land use: Distant drivers of land change and geographic displacement of land use. *Curr. Opin. Environ. Sustain.* **2013**, *5*, 438–444. [CrossRef]

4. Mottet, A.; Ladet, S.; Coqué, N.; Gibon, A. Agricultural land-use change and its drivers in mountain landscapes: A case study in the Pyrenees. *Agric. Ecosyst. Environ.* **2006**, *114*, 296–310. [CrossRef]
5. Amici, V.; Marcantonio, M.; La Porta, N.; Rocchini, D. A multi-temporal approach in MaxEnt modelling: A new frontier for land use/land cover change detection. *Ecol. Inform.* **2017**, *40*, 40–49. [CrossRef]
6. Jongman, R.H.G. Homogenisation and fragmentation of the European landscape: Ecological consequences and solutions. *Landsc. Urban Plan.* **2002**, *58*, 211–221. [CrossRef]
7. Zhai, R.; Zhang, C.; Allen, J.M.; Li, W.; Boyer, M.A.; Segerson, K.; Foote, K.E. Predicting land use/cover change in Long Island Sound Watersheds and its effect on invasive species: A case study for glossy buckthorn. *Ann. GIS* **2018**, *24*, 83–97. [CrossRef]
8. Chouvardas, D.; Karatassiou, M.; Stergiou, A.; Chrysanthopoulou, G. Identifying the Spatiotemporal Transitions and Future Development of a Grazed Mediterranean Landscape of South Greece. *Land* **2022**, *11*, 2141. [CrossRef]
9. Polasky, S.; Nelson, E.; Pennington, D.; Johnson, K.A. The Impact of Land-Use Change on Ecosystem Services, Biodiversity and Returns to Landowners: A Case Study in the State of Minnesota. *Environ. Resour. Econ.* **2011**, *48*, 219–242. [CrossRef]
10. Yang, S.; Zhao, W.; Liu, Y.; Wang, S.; Wang, J.; Zhai, R. Influence of land use change on the ecosystem service trade-offs in the ecological restoration area: Dynamics and scenarios in the Yanhe watershed, China. *Sci. Total Environ.* **2018**, *644*, 556–566. [CrossRef]
11. Pelorosso, R.; Leone, A.; Boccia, L. Land cover and land use change in the Italian central Apennines: A comparison of assessment methods. *Appl. Geogr.* **2009**, *29*, 35–48. [CrossRef]
12. Rivas-Martínez, S.; Penas, Á.; Díaz González, T.E.; Cantó, P.; del Río, S.; Costa, J.C.; Herrero, L.; Molero, J. Biogeographic Units of the Iberian Peninsula and Baelaric Islands to District Level. A Concise Synopsis. In *The Vegetation of the Iberian Peninsula: Volume 1*; Loidi, J., Ed.; Springer International Publishing: Cham, Switzerland, 2017; pp. 131–188.
13. Williams, A.P.; Allen, C.D.; Macalady, A.K.; Griffin, D.; Woodhouse, C.A.; Meko, D.M.; Swetnam, T.W.; Rauscher, S.A.; Seager, R.; Grissino-Mayer, H.D.; et al. Temperature as a potent driver of regional forest drought stress and tree mortality. *Nat. Clim. Chang.* **2013**, *3*, 292–297. [CrossRef]
14. Guisan, A.; Tingley, R.; Baumgartner, J.B.; Naujokaitis-Lewis, I.; Sutcliffe, P.R.; Tulloch, A.I.T.; Regan, T.J.; Brotons, L.; McDonald-Madden, E.; Mantyka-Pringle, C.; et al. Predicting species distributions for conservation decisions. *Ecol. Lett.* **2013**, *16*, 1424–1435. [CrossRef] [PubMed]
15. del Río, S.; Canas, R.; Cano, E.; Cano-Ortiz, A.; Musarella, C.; Pinto-Gomes, C.; Penas, A. Modelling the impacts of climate change on habitat suitability and vulnerability in deciduous forests in Spain. *Ecol. Indic.* **2021**, *131*, 108202. [CrossRef]
16. IPCC. *Mitigation of Climate Change. Contribution of Working Group III to the Fifth Assessment Report of the Intergovernmental Panel on Climate Change*; Edenhofer, O., Pichs-Madruga, R., Sokona, Y., Farahani, E., Kadner, S., Seyboth, K., Adler, A., Baum, I., Brunner, S., Eickemeier, P., et al., Eds.; Cambridge University Press: Cambridge, NY, USA, 2014.
17. Worth, J.R.P.; Harrison, P.A.; Williamson, G.J.; Jordan, G.J. Whole range and regional-based ecological niche models predict differing exposure to 21st century climate change in the key cool temperate rainforest tree southern beech (*Nothofagus cunninghamii*). *Austral Ecol.* **2015**, *40*, 126–138. [CrossRef]
18. IPCC. *Climate Change 2021: The Physical Basis. Contribution of Working Group I to the Sixth Assessment Report of the Intergovernmental Panel on Climate Change*; Masson-Delmotte, V., Zhai, P., Pirani, A., Connors, S.L., Péan, C., Berger, S., Caud, N., Chen, Y., Goldfarb, L., Gomis, M.I., et al., Eds.; Cambridge University Press: Cambridge, NY, USA, 2021.
19. Purohit, S.; Rawat, N. MaxEnt modeling to predict the current and future distribution of *Clerodendrum infortunatum* L. under climate change scenarios in Dehradun district, India. *Model. Earth Syst. Environ.* **2022**, *8*, 2051–2063. [CrossRef]
20. Warren, R.; VanDerWal, J.; Price, J.; Welbergen, J.A.; Atkinson, I.; Ramirez-Villegas, J.; Osborn, T.J.; Jarvis, A.; Shoo, L.P.; Williams, S.E.; et al. Quantifying the benefit of early climate change mitigation in avoiding biodiversity loss. *Nat. Clim. Chang.* **2013**, *3*, 678–682. [CrossRef]
21. Qin, A.; Liu, B.; Guo, Q.; Bussmann, R.W.; Ma, F.; Jian, Z.; Xu, G.; Pei, S. Maxent modeling for predicting impacts of climate change on the potential distribution of *Thuja sutchuenensis* Franch., an extremely endangered conifer from southwestern China. *Glob. Ecol. Conserv.* **2017**, *10*, 139–146. [CrossRef]
22. Muhammad, R.; Zhang, W.; Abbas, Z.; Guo, F.; Gwiazdzinski, L. Spatiotemporal Change Analysis and Prediction of Future Land Use and Land Cover Changes Using QGIS MOLUSCE Plugin and Remote Sensing Big Data: A Case Study of Linyi, China. *Land* **2022**, *11*, 419. [CrossRef]
23. Phillips, S.J.; Anderson, R.P.; Schapire, R.E. Maximum entropy modeling of species geographic distributions. *Ecol. Model.* **2006**, *190*, 231–259. [CrossRef]
24. Elith, J.; Graham, C.H. Do they? How do they? WHY do they differ? On finding reasons for differing performances of species distribution models. *Ecography* **2009**, *32*, 66–77. [CrossRef]
25. Peterson, A.T.; Papeş, M.; Eaton, M. Transferability and model evaluation in ecological niche modeling: A comparison of GARP and Maxent. *Ecography* **2007**, *30*, 550–560. [CrossRef]
26. Warren, D.L.; Seifert, S.N. Ecological niche modeling in Maxent: The importance of model complexity and the performance of model selection criteria. *Ecol. Appl.* **2011**, *21*, 335–342. [CrossRef] [PubMed]
27. Cao, Y.T.; Lu, Z.P.; Gao, X.Y.; Liu, M.L.; Sa, W.; Liang, J.; Wang, L.; Yin, W.; Shang, Q.H.; Li, Z.H. Maximum Entropy Modeling the Distribution Area of Morchella Dill. ex Pers. Species in China under Changing Climate. *Biology* **2022**, *11*, 1027. [CrossRef]

28. Helmstetter, N.A.; Conway, C.J.; Stevens, B.S.; Goldberg, A.R. Balancing transferability and complexity of species distribution models for rare species conservation. *Divers. Distrib.* **2021**, *27*, 95–108. [CrossRef]
29. Pandit, P.R.; Fulekar, M.H.; Karuna, M.S.L. Effect of salinity stress on growth, lipid productivity, fatty acid composition, and biodiesel properties in *Acutodesmus obliquus* and *Chlorella vulgaris*. *Environ. Sci. Pollut. Res. Int.* **2017**, *24*, 13437–13451. [CrossRef]
30. Hemati, T.; Pourebrahim, S.; Monavari, M.; Baghvand, A. Species-specific nature conservation prioritization (a combination of MaxEnt, Co$ting Nature and DINAMICA EGO modeling approaches). *Ecol. Model.* **2020**, *429*, 109093. [CrossRef]
31. Xiong, Q.; Luo, X.; Liang, P.; Xiao, Y.; Xiao, Q.; Sun, H.; Pan, K.; Wang, L.; Li, L.; Pang, X. Fire from policy, human interventions, or biophysical factors? Temporal–spatial patterns of forest fire in southwestern China. *For. Ecol. Manag.* **2020**, *474*, 118381. [CrossRef]
32. Bosso, L.; Ancillotto, L.; Smeraldo, S.; D'Arco, S.; Migliozzi, A.; Conti, P.; Russo, D. Loss of potential bat habitat following a severe wildfire: A model-based rapid assessment. *Int. J. Wildland Fire* **2018**, *27*, 756–769. [CrossRef]
33. Yoshimura, N.; Hiura, T. Demand and supply of cultural ecosystem services: Use of geotagged photos to map the aesthetic value of landscapes in Hokkaido. *Ecosyst. Serv.* **2017**, *24*, 68–78. [CrossRef]
34. Thonfeld, F.; Steinbach, S.; Muro, J.; Kirimi, F. Long-Term Land Use/Land Cover Change Assessment of the Kilombero Catchment in Tanzania Using Random Forest Classification and Robust Change Vector Analysis. *Remote Sens.* **2020**, *12*, 1057. [CrossRef]
35. Li, Z.; Liu, Y.; Zeng, H. Application of the MaxEnt model in improving the accuracy of ecological red line identification: A case study of Zhanjiang, China. *Ecol. Indic.* **2022**, *137*, 108767. [CrossRef]
36. Saha, A.; Rahman, S.; Alam, S. Modeling current and future potential distributions of desert locust *Schistocerca gregaria* (Forskål) under climate change scenarios using MaxEnt. *J. Asia-Pac.* **2021**, *14*, 399–409. [CrossRef]
37. Mack, B.; Roscher, R.; Stenzel, S.; Feilhauer, H.; Schmidtlein, S.; Waske, B. Mapping raised bogs with an iterative one-class classification approach. *ISPRS J. Photogramm. Remote Sens. I* **2016**, *120*, 53–64. [CrossRef]
38. FAO. *Global Forest Resources Assessment 2010*; FAO: Rome, Italy, 2010; Volume 163, p. 340.
39. White, R.P.; Murray, S.; Rohweder, M. Pilot Analysis of Global Ecosystems: Grassland Ecosystems. World Resources Institute: Washington, DC, USA, 2000; p. 81.
40. Reynolds, J.F.; Smith, D.M.S.; Lambin, E.F.; Turner, B.L.; Mortimore, M.; Batterbury, S.P.J.; Downing, T.E.; Dowlatabadi, H.; Fernández, R.J.; Herrick, J.E. Global desertification: Building a science for dryland development. *Science* **2007**, *316*, 847–851. [CrossRef] [PubMed]
41. Neely, M.E.; Schallert, D.L.; Mohammed, S.S.; Roberts, R.M.; Chen, Y.J. Self-kindness when facing stress: The role of self-compassion, goal regulation, and support in college students' well-being. *Motiv. Emot.* **2009**, *33*, 88–97. [CrossRef]
42. Allen-Diaz, B.; Chapin, F.S.; Diaz, S.; Howden, M.; Puidefabregas, J.; Stafford, M.; Benning, T.; Bryant, F.; Campbell, B.; duToit, J. Grassland and rangelands. In *Climate Change 1995: Impacts, Adaptations, and Mitigation of Climate Change: Scientific-Technical Analyses. Contribution of Working Group II to the Second Assessment Report of the Intergovernmental Panel on Climate Change*; Watson, R.T., Zinyowera, M.C., Moss, R.H., Eds.; Cambridge Univ. Press: Cambridge, UK; New York, NY, USA, 1996; p. 878.
43. Olff, H.; Ritchie, M.E.; Prins, H.H.T. Global environmental controls of diversity in large herbivores. *Nature* **2002**, *415*, 901–904. [CrossRef]
44. Alkemade, R.; Reid, R.S.; van den Berg, M.; de Leeuw, J.; Jeuken, M. Assessing the impacts of livestock production on biodiversity in rangeland ecosystems. *Proc. Natl. Acad. Sci. USA* **2013**, *110*, 20900–20905. [CrossRef]
45. Hayati, D.; Ranjbar, Z.; Karami, E. Measuring agricultural sustainability. In *Biodiversity, Biofuels, Agroforestry and Conservation Agriculture*; Springer: Dordrecht, The Netherlands, 2011; pp. 73–100. [CrossRef]
46. Straffelini, E.; Luo, J.; Tarolli, P. Climate change is threatening mountain grasslands and their cultural ecosystem services. *Catena* **2024**, *237*, 107802. [CrossRef]
47. Liu, Y.; Dong, J.; Ren, S.; Liu, Y. Differential impacts of degradation on grassland ecosystems in the Tibetan Plateau and the Northern agro-pastoral ecotone: A meta-analysis. *Plant Soil* **2024**, *496*, 677–696. [CrossRef]
48. Gibson, D.J.; Newman, J.A. Grasslands and climate change: An overview. In *Grasslands and Climate Change*; Gibson, D.J., Newman, J.A., Eds.; Ecological Reviews; Cambridge University Press: Cambridge, NY, USA, 2019; pp. 3–18.
49. Bond, W.J.; Keeley, J.E. Fire as a global 'herbivore': The ecology and evolution of flammable ecosystems. *Trends Ecol. Evol.* **2005**, *20*, 387–394. [CrossRef] [PubMed]
50. Middleton, N.J. Rangeland management and climate hazards in drylands: Dust storms, desertification and the overgrazing debate. *Nat. Hazards Obs.* **2018**, *92*, 57–70. [CrossRef]
51. Middleton, N.J.; Sternberg, T. Climate hazards in drylands: A review. *Earth-Sci. Rev.* **2013**, *126*, 48–57. [CrossRef]
52. Reid, W.V.; Mooney, H.; Cropper, A.; Capistrano, D.; Carpenter, S.R.; Chopra, K.R.; Dasgupta, P.; Dietz, T.; Duraiappah, A.K.; Hassan, R.M.; et al. *Millennium Ecosystem Assessment, 2005. Ecosystem and Human Well-being:Synthesis*; Island Press: Wasinghton, DC, USA, 2005; p. 156.
53. Eteraf, H.; Telvari, A.A.R. Effects of animal grazing on some physical characteristics of loose soil in Maravetapeh rangelands, Golestan, Iran. *Pajouhesh-Va-Sazandegi* **2005**, *17*, 8–13.
54. Rahmati, O.; Samani, A.N.; Mahmoodi, N.; Mahdavi, M. Assessment of the Contribution of N-Fertilizers to Nitrate Pollution of Groundwater in Western Iran (Case Study: Ghorveh–Dehgelan Aquifer). *Water Qual. Expo. Health* **2015**, *7*, 143–151. [CrossRef]
55. Maruşca, T.; Roman, A.; Taulescu, E. Detecting trends in the quality and productivity of grasslands by analyzing the historical vegetation relevés: A case study from Southeastern Carpathians, Vlădeasa Mountains (Romania). *Not. Bot. Horti Agrobot.* **2021**, *49*, 12378. [CrossRef]

56. Wu, Y.; Du, Y.; Liu, X.; Wan, X.; Yin, B.; Hao, Y.; Wang, Y.S. Grassland biodiversity response to livestock grazing, productivity, and climate varies across biome components and diversity measurements. *Sci. Total Environ.* **2023**, *878*, 162994. [CrossRef] [PubMed]
57. Karatassiou, M.; Parissi, Z.M.; Panajiotidis, S.; Stergiou, A. Impact of Grazing on Diversity of Semi-Arid Rangelands in Crete Island in the Context of Climatic Change. *Plants* **2022**, *11*, 982. [CrossRef]
58. Blondel, J. *The Mediterranean Region: Biological Diversity in Space and Time*; Oxford University Press: Oxford, UK, 2010.
59. Papachristou, T.G.; Ispikoudis, I.P. Multifunctionality of rangelands and its relevance to the development of mountainous and less favoured areas. In *Range Science and Development of Mountainous Regions, Proceedings of the 3rd Panhellenic Rangeland Congress, Karpenissi, Greece, 4–6 September 2002*; Hellenic Range & Pasture Society: Athens, Greece, 2003; pp. 13–23, (in Greek with English abstract).
60. Kyriazopoulos, A.P.; Karatassiou, M.; Parissi, Z.M.; Abraham, E.M.; Sklavou, P. Effects of Ski-Resort Activities and Transhumance Livestock Grazing on Rangeland Ecosystems of Mountain Zireia, Southern Greece. *Land* **2022**, *11*, 1462. [CrossRef]
61. Ragkos, A. Transhumance in Greece: Multifunctionality as an Asset for Sustainable Development. In *Grazing Communities*; Letizia, B., Ed.; Berghahn Books: New York, NY, USA; Oxford, UK, 2022; pp. 23–43.
62. Bravo, D.N.; Araújo, M.B.; Lasanta, T.; Moreno, J.I.L. Climate Change in Mediterranean Mountains during the 21st Century. *AMBIO J. Hum. Environ.* **2008**, *37*, 280–285. [CrossRef]
63. Peters, D.P.C.; Yao, J.; Sala, O.E.; Anderson, J.P. Directional climate change and potential reversal of desertification in arid and semiarid ecosystems. *Glob. Chang. Biol.* **2012**, *18*, 151–163. [CrossRef]
64. Chrysanthopoulou, G. *Synergy of Climate and Grazing in the Evolution of Vegetation on Mount Kyllini*; Aristotle University of Thessaloniki: Thessaloniki, Greece, 2021.
65. Zhou, Y.; Zhang, Z.; Zhu, B.; Cheng, X.; Yang, L.; Gao, M.; Kong, R. MaxEnt Modeling Based on CMIP6 Models to Project Potential Suitable Zones for Cunninghamia lanceolata in China. *Forests* **2021**, *12*, 752. [CrossRef]
66. Feng, X.; Park, D.S.; Liang, Y.; Pandey, R.; Papeş, M. Collinearity in ecological niche modeling: Confusions and challenges. *Ecol. Evol.* **2019**, *9*, 10365–10376. [CrossRef] [PubMed]
67. Elith, J.; Phillips, S.J.; Hastie, T.; Dudík, M.; Chee, Y.E.; Yates, C.J. A statistical explanation of MaxEnt for ecologists. *Divers. Distrib.* **2011**, *17*, 43–57. [CrossRef]
68. Hu, W.; Wang, Y.S.; Zhang, D.; Yu, W.; Chen, G.; Xie, T.; Liu, Z.; Ma, Z.; Du, J.; Chao, B.; et al. Mapping the potential of mangrove forest restoration based on species distribution models: A case study in China. *Sci. Total Environ.* **2020**, *748*, 142321. [CrossRef]
69. De Marco, P.J.; Nóbrega, C.C. Evaluating collinearity effects on species distribution models: An approach based on virtual species simulation. *PLoS ONE* **2018**, *13*, e0202403. [CrossRef]
70. Luna, S.; Peña-Peniche, A.; Mendoza-Alfaro, R. Species distribution model accuracy is strongly influenced by the choice of calibration area. *Biodivers. Inform.* **2024**, *18*, 43–55. [CrossRef]
71. Voldoire, A.; Saint-Martin, D.; Sénési, S.; Decharme, B.; Alias, A.; Chevallier, M.; Colin, J.; Guérémy, J.-F.; Michou, M.; Moine, M.-P.; et al. Evaluation of CMIP6 DECK Experiments With CNRM-CM6-1. *J. Adv. Model. Earth Syst.* **2019**, *11*, 2177–2213. [CrossRef]
72. Cherchi, A.; Fogli, P.G.; Lovato, T.; Peano, D.; Iovino, D.; Gualdi, S.; Masina, S.; Scoccimarro, E.; Materia, S.; Bellucci, A.; et al. Global Mean Climate and Main Patterns of Variability in the CMCC-CM2 Coupled Model. *J. Adv. Model. Earth Syst.* **2019**, *11*, 185–209. [CrossRef]
73. Lovato, T.; Peano, D.; Butenschön, M.; Materia, S.; Iovino, D.; Scoccimarro, E.; Fogli, P.G.; Cherchi, A.; Bellucci, A.; Gualdi, S.; et al. CMIP6 Simulations With the CMCC Earth System Model (CMCC-ESM2). *J. Adv. Model. Earth Syst.* **2022**, *14*, e2021MS002814. [CrossRef]
74. Riahi, K.; van Vuuren, D.P.; Kriegler, E.; Edmonds, J.; O'Neill, B.C.; Fujimori, S.; Bauer, N.; Calvin, K.; Dellink, R.; Fricko, O.; et al. The Shared Socioeconomic Pathways and their energy, land use, and greenhouse gas emissions implications: An overview. *Glob. Environ. Chang.* **2017**, *42*, 153–168. [CrossRef]
75. Carozzi, M.; Martin, R.; Klumpp, K.; Massad, R.S. Effects of climate change in European croplands and grasslands: Productivity, greenhouse gas balance and soil carbon storage. *Biogeosciences* **2022**, *19*, 3021–3050. [CrossRef]
76. Yan, H.; Feng, L.; Zhao, Y.; Feng, L.; Wu, D.; Zhu, C. Prediction of the spatial distribution of *Alternanthera philoxeroides* in China based on ArcGIS and MaxEnt. *Glob. Ecol. Conserv.* **2020**, *21*, e00856. [CrossRef]
77. Abolmaali, S.M.R.; Tarkesh, M.; Bashari, H. MaxEnt modeling for predicting suitable habitats and identifying the effects of climate change on a threatened species, *Daphne mucronata*, in central Iran. *Ecol. Inform.* **2018**, *43*, 116–123. [CrossRef]
78. Duan, X.; Li, J.; Wu, S. MaxEnt Modeling to Estimate the Impact of Climate Factors on Distribution of Pinus densiflora. *Forests* **2022**, *13*, 402. [CrossRef]
79. Tavanpour, T.; Sarafrazi, A.; Mehrnejad, M.R.; Imani, S. Distribution modelling of Acrosternum spp. (Hemiptera: Pentatomidae) in south of Iran. *Biologia* **2019**, *74*, 1627–1635. [CrossRef]
80. Ramasamy, M.; Das, B.; Ramesh, R. Predicting climate change impacts on potential worldwide distribution of fall armyworm based on CMIP6 projections. *J. Pest Sci.* **2022**, *95*, 841–854. [CrossRef]
81. Yang, X.Q.; Kushwaha, S.P.S.; Saran, S.; Xu, J.; Roy, P.S. Maxent modeling for predicting the potential distribution of medicinal plant, Justicia adhatoda L. in Lesser Himalayan foothills. *Ecol. Eng.* **2013**, *51*, 83–87. [CrossRef]
82. Wei, X.; Zhu, C.; Xiao, K.; Yin, Q.; Zha, Y. Shortest Path Network Interdiction With Goal Threshold. *IEEE Access* **2018**, *6*, 29332–29343. [CrossRef]

83. Wang, Y.S.; Xie, B.Y.; Wan, F.H.; Xiao, Q.M.; Dai, L.Y. The Potential Geographic Distribution of Radopholus similis in China. *Agric. Sci. China* **2007**, *6*, 1444–1449. [CrossRef]
84. Coban, O.; Örücü, Ö.K.; Arslan, E. MaxEnt Modeling for Predicting the Current and Future Potential Geographical Distribution of Quercus libani Olivier. *Sustainability* **2020**, *12*, 2671. [CrossRef]
85. Fielding, A.H. A review of methods for the assessment of prediction errors in conservation presence/absence models. *Environ. Conserv.* **1997**, *24*, 38–49. [CrossRef]
86. Peavey, L. Predicting pelagic habitat with presence-only data using maximum entropy for olive ridley sea turtles in the Eastern Tropical Pacific in the Eastern Tropical Pacific. Master's Thesis, Duke University, Durham, NC, USA, 2010.
87. Thuiller, W.; Richardson, D.M.; Rouget, M.; Procheş, Ş.; Wilson, J.R.U. Interactions between environment, species traits, and human uses describe patterns of plant invasions. *Ecology* **2006**, *87*, 1755–1769. [CrossRef]
88. Buckman-Sewald, J.; Whorton, C.R.; Root, K.V. Developing macrohabitat models for bats in parks using maxent and testing them with data collected by citizen scientists. *Int. J. Biodivers. Conserv.* **2014**, *6*, 171–183. [CrossRef]
89. Jaskowiak, P.A.; Costa, I.G.; Campello, R.J.G.B. The area under the ROC curve as a measure of clustering quality. *Data Min. Knowl. Discov.* **2022**, *36*, 1219–1245. [CrossRef]
90. Shi, X.; Wang, J.; Zhang, L.; Chen, S.; Zhao, A.; Ning, X.; Fan, G.; Wu, N.; Zhang, L.; Wang, Z. Prediction of the potentially suitable areas of *Litsea cubeba* in China based on future climate change using the optimized MaxEnt model. *Ecol. Indic.* **2023**, *148*, 110093. [CrossRef]
91. Bede-Fazekas, Á.; Somodi, I. Precipitation and temperature timings underlying bioclimatic variables rearrange under climate change globally. *Glob. Chang. Biol.* **2024**, *30*, e17496. [CrossRef]
92. Hawkins, E.; Sutton, R. The potential to narrow uncertainty in projections of regional precipitation change. *Clim. Dyn.* **2011**, *37*, 407–418. [CrossRef]
93. Wang, Z.; Li, X.; Mao, Y.; Li, L.; Wang, X.; Lin, Q. Dynamic simulation of land use change and assessment of carbon storage based on climate change scenarios at the city level: A case study of Bortala, China. *Ecol. Indic.* **2022**, *134*, 108499. [CrossRef]
94. Zhang, Y.; Tang, J.; Ren, G.; Zhao, K.; Wang, X. Global potential distribution prediction of *Xanthium italicum* based on Maxent model. *Sci. Rep.* **2021**, *11*, 16545. [CrossRef]
95. Inouye, D.W. Climate change and phenology. *WIREs Clim. Chang.* **2022**, *13*, e764. [CrossRef]
96. Auffret, A.G. Historical floras reflect broad shifts in flowering phenology in response to a warming climate. *Ecosphere* **2021**, *12*, e03683. [CrossRef]
97. Currier, C.M.; Sala, O.E. Precipitation versus temperature as phenology controls in drylands. *Ecology* **2022**, *103*, e3793. [CrossRef]
98. Nemani, R.R.; Keeling, C.D.; Hashimoto, H.; Jolly, W.M.; Piper, S.C.; Tucker, J.; Myneni, R.B.; Running, S.W. Climate-driven increases in global terrestrial net primary production from 1982 to 1999. *Science* **2003**, *300*, 1560–1563. [CrossRef]
99. Gibson, D.J. *Grasses and Grassland Ecology*; Oxford University Press: Oxford, UK, 2009.
100. Xun, Q.; An, S.; Lu, M. Climate change and topographic differences influence grassland vegetation greening across environmental gradients. *Front. Environ. Sci.* **2024**, *11*, 1324742. [CrossRef]
101. Cui, N.; Luo, G.; Du, S. Analysis of Spatial-Temporal Variation of Grassland Landscape Pattern Based on Terrain Factors in Qinghai Yushu Tibetan Autonomous Prefecture, China. In Proceedings of the 2018 26th International Conference on Geoinformatics, Kunming, China, 28–30 June 2018; pp. 1–7.
102. Ye, J.; Ji, Y.; Wang, J.; Ma, X.; Gao, J. Climate factors dominate the elevational variation in grassland plant resource utilization strategies. *Front. Environ. Sci.* **2024**, *15*, 1430027. [CrossRef]
103. Rayamajhi, N.; Manandhar, B. Impact of Climate Change and Adaptation Measures on Transhumance Herding System in Gatlang, Rasuwa. *Air Soil Water Res.* **2020**, *13*, 1178622120951173. [CrossRef]
104. Bhatta, L.D.; Udas, E.; Khan, B.; Ajmal, A.; Amir, R.; Ranabhat, S. Local knowledge based perceptions on climate change and its impacts in the Rakaposhi valley of Gilgit-Baltistan, Pakistan. *Int. J. Clim. Chang. Strateg. Manag.* **2020**, *12*, 222–237. [CrossRef]
105. Satti, Z.; Naveed, M.; Shafeeque, M.; Li, L. Investigating the impact of climate change on trend shifts of vegetation growth in Gilgit Baltistan. *Glob. Planet. Chang.* **2024**, *232*, 104341. [CrossRef]
106. Kiziridis, D.A.; Mastrogianni, A.; Pleniou, M.; Karadimou, E.; Tsiftsis, S.; Xystrakis, F.; Tsiripidis, I. Acceleration and relocation of abandonment in a Mediterranean mountainous landscape: Drivers, consequences, and management implications. *Land* **2022**, *11*, 406. [CrossRef]
107. Karatassiou, M.; Parissi, Z.M.; Stergiou, A.; Chouvardas, D.; Mantzanas, K. Patterns of transhumant livestock system on Mount Zireia, Peloponnese, Greece. In Proceedings of the Pastoralism and Sustainable Development, Valenzano, Bari, 14–15 July 2021; pp. 197–200.
108. Sidiropoulou, A.; Chouvardas, D.; Mantzanas, K.; Stefanidis, S.; Karatassiou, M. Impact of Transhumant Livestock Grazing Abandonment on Pseudo-Alpine Grasslands in Greece in the Context of Climatic Change. *Land* **2022**, *11*, 2126. [CrossRef]
109. Almeida, A.M.; Martins, M.J.; Campagnolo, M.L.; Fernandez, P.; Albuquerque, T.; Gerassis, S.; Gonçalves, J.C.; Ribeiro, M.M. Prediction scenarios of past, present, and future environmental suitability for the Mediterranean species *Arbutus unedo* L. *Sci. Rep.* **2022**, *12*, 84. [CrossRef]
110. Almeida, A.M.; Ribeiro, M.M.; Ferreira, M.R.; Roque, N.; Quintela-Sabarís, C.; Fernandez, P. Big data help to define climate change challenges for the typical Mediterranean species *Cistus ladanifer* L. *Front. Ecol. Evol.* **2023**, *11*, 1136224. [CrossRef]

111. Chan, D.; Cobb, A.; Zeppetello, L.R.V.; Battisti, D.S.; Huybers, P. Summertime Temperature Variability Increases With Local Warming in Midlatitude Regions. *Geophys. Res. Lett.* **2020**, *47*, e2020GL087624. [CrossRef]
112. Adler, P.B.; Levine, J.M. Contrasting relationships between precipitation and species richness in space and time. *Oikos* **2007**, *116*, 221–232. [CrossRef]
113. Herrero-Jáuregui, C.; Oesterheld, M. Effects of grazing intensity on plant richness and diversity: A meta-analysis. *Oikos* **2018**, *127*, 757–766. [CrossRef]
114. Zhang, K.; Zhang, Y.; Zhou, C.; Meng, J.; Sun, J.; Zhou, T.; Tao, J. Impact of climate factors on future distributions of *Paeonia ostii* across China estimated by MaxEnt. *Ecol. Inform.* **2019**, *50*, 62–67. [CrossRef]
115. Koerner, S.E.; Burkepile, D.E.; Fynn, R.W.S.; Burns, C.E.; Eby, S.; Govender, N.; Hagenah, N.; Matchett, K.J.; Thompson, D.I.; Wilcox, K.R.; et al. Plant community response to loss of large herbivores differs between North American and South African savanna grasslands. *Ecology* **2014**, *95*, 808–816. [CrossRef]
116. Pinto-Junior, H.V.; Villa, P.M.; de Menezes, L.T.; Pereira, M.C.A. Effect of climate and altitude on plant community composition and richness in Brazilian inselbergs. *J. Mt. Sci.* **2020**, *17*, 1931–1941. [CrossRef]